Proceedings of the 8th International Conference on MicroManufacturing
University of Victoria, Victoria, BC, Canada, March 25-28, 2013

Micro-EDM Pulse Energy Distribution Ratio Determination

ICOMM 2013 No.20

Bai Shao[1], Kamlakar P. Rajurkar[2]

[1]Bai Shao; MME department, University of Nebraska-Lincoln, USA; bshao@huskers.unl.edu•
[2]Kamlakar P. Rajurkar; MME department, University of Nebraska-Lincoln, USA; krajurkar1@unl.edu

Key Words: micro-EDM, pulse energy distribution, modeling

ABSTRACT

In this paper, a method for determining pulse energy distribution ratio in micro-EDM is presented. The pulse energy distribution ratio is a critical parameter in the EDM process. It determines how much of the total energy of a pulse has been distributed into each electrode and the inter-electrode gap. Instead of measuring the electrode temperature variation (which is very difficult), the method in this paper uses the dimensions of the generated craters to determine the pulse energy distribution ratio. The semi-infinite body with uniform disk heat source conduction model has been applied to simulate the EDM erosion process. By solving the thermal model, the radius of the plasma and the pulse energy distribution ratio can be got. Experiments with the pulse energy from 0.09 μJ to 1.02 μJ show that, the average pulse energy distribution ratio is 9.4% to the anode and is 3.6% to the cathode, respectively. These results agree with other reported EDM literature. Additionally the relationship of the anode crater volume to pulse energy is found to be linear.

INTRODUCTION

Micro-EDM is a nontraditional machining process that removes material by rapidly occurring electric sparks between two electrodes submerged in dielectric fluid. However, because of the complexity of this electrical thermal process, erosion mechanism including energy distribution into the electrodes is not yet fully understood.

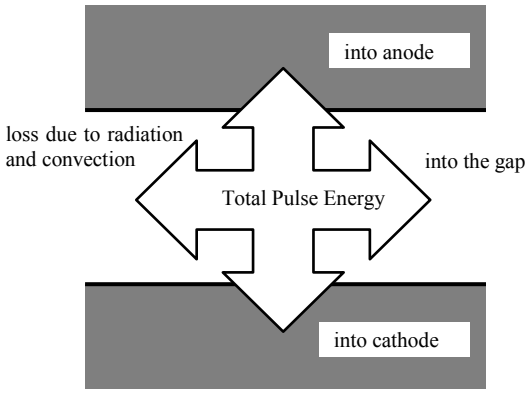

Fig. 1: Distribution of pulse energy

In EDM, even if the anode and cathode materials are the same, the amount of material removed from each electrode is still quite different. This phenomenon is due to the difference in pulse energy distributed into the electrodes [1]. After a pulse occurs, the pulse energy is distributed to the electrodes and the inter-electrode gap, and some portion of the energy is also lost due to radiation and convection. Fig. 1 shows the distribution of the pulse energy.

It is crucial to know the energy distribution ratio in the EDM process. Firstly, in industry, by adjusting the pulse energy distribution ratio, a better machining performance can be obtained. Because, the single spark removal amount highly depends on the energy distributed into the electrodes in EDM [2]. When pulse energy is fixed, a larger fraction of energy is distributed into the workpiece which leads to more removal, which in turn could increase the efficiency of the EDM process. Conversely, a lower fraction of the energy is distributed into the tool electrode which leads to less removal, which in turn could prolong the tool life and increase the accuracy of the process. Secondly, in research, the energy distribution ratio is a critical parameter in all EDM models. The accuracy of theoretical models [2-6] are based on the pulse energy distribution ratio. These models have been established to explain the phenomenon and predict the performance of process, such as the formation of craters, material removal rate (MRR), and electrode wear ratio (EWR).

To determine this ratio, a method by using thermocouples to measure the temperature variation of electrodes in the EDM has been widely applied [7-9]. This method has also been extended to the micro-EMD. In paper [10], authors are using multiple sparks instead of a single spark to make the temperature change of electrodes measurable. However, the temperature measurement method is not easy to apply because it requires mounting transducers and other special equipment to the machine. Especially in micro-EDM, the size effect makes it even harder to apply. Therefore, some researchers [4-6] are using the values from other papers, which may not fit their working conditions well. J Tao et al. [4] have stated that one possible way of improving their work could be revising the parameter values, which the authors are getting from others literature, to fit their working conditions. Therefore, industry and research expect an easy and accurate method to determine the energy distribution ratio.

In this paper, a method for determining pulse energy distribution ratio in micro-EDM is presented. Based on the uniform disk heat source conduction model, this method uses the dimensions of the generated craters to determine the energy distribution ratio. Measured radius and depth of the crater is used to find the energy distribution ratio and the plasma radius.

• corresponding author. mailing address: W340 NH, Lincoln, NE, 68588, USA. phone: (919) 260-3746. e-mail: bshao@huskers.unl.edu.

THERMAL MODEL FOR SINGLE SPARK MICRO-EDM

A. AUSSMPTIONS

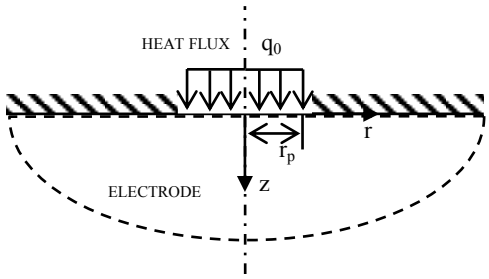

Fig. 2: Semi-infinite body with uniform heat flux model

The method for determining pulse energy distribution ratio is based on the semi-infinite body with uniform heat flux conduction model. Fig. 2 shows the schematic of this model, where a uniform distributed heat flux q_0 with a fixed radius r_p is applied.

To make this model valid for the EDM process, following assumptions are made.

1. Only one spark is occurring for each discharge.
2. Pulse energy is contributed by the current and voltage.
3. Pulse energy is distributed into the electrodes only by conduction heat transfer.
4. Heat loss from the electrodes is insignificant.
5. Plasma channel is a fixed circular column, and the heat flux of the electrode surface within the plasma is uniform distributed.
6. Heat transfer through the electrode is 2-dimensional.
7. Pulse energy distribution ratio is a constant value during discharge.
8. Average thermophysical properties are applied over the entire temperature range. (See Table 1.)
9. The latent heat of phase change is neglected.
10. Material hotter than the melting point will be removed after the discharge.

With all these assumptions, the model has been proven valid for both EDM and micro-EDM processes [2, 3].

Table 1: Thermophysical properties of Ti -6Al-4V

Thermophysical properties value	
Density	: 4.42(g/cm^3)
Melting point	: 1,649(℃)
Average specific heat	: 560(J/Kg · ℃)
Average thermal conductivity	: 7.2(W/m · K)

B. THERMAL MODEL

The governing equation of this heat transfer model is given by the partial differential equation (PDE) below,

$$\frac{1}{r}\frac{\partial}{\partial r}\left(r\frac{\partial T}{\partial r}\right)+\frac{\partial^2 T}{\partial z^2}=\frac{1}{\alpha}\frac{\partial T}{\partial t}. \tag{1}$$

The boundary conditions are

$$-k\frac{\partial T(r,0,t)}{\partial z}=\begin{cases}q_0; & for\ 0\le r\le r_p\\ 0; & for\ r>r_p,\end{cases} \tag{2}$$

$$T(\infty,\infty,t)=20\ ℃. \tag{3}$$

And the initial condition is

$$T(r,z,0)=20\ ℃. \tag{4}$$

Where r and z are the radius and depth in cylindrical coordinates; t is the time; T is the temperature; α is the diffusivity; k is the conductivity; r_p is the plasma radius, and q_0 is the heat flux.

The exact solution [11] of this PDE is given by

$$\begin{aligned}T(r,z,t)=\frac{1}{2}\frac{q_o r_p}{k}\int_{\beta=0}^{\infty}J_0\left(\frac{\beta r}{r_p}\right)J_1(\beta)\\ \times\left(e^{-\beta z/r_p}\left\{1+erf\left[\frac{\beta\sqrt{\alpha t}}{r_p}-\frac{z}{2\sqrt{\alpha t}}\right]\right\}\right.\\ \left.-e^{\beta z/r_p}erfc\left[\frac{\beta\sqrt{\alpha t}}{r_p}+\frac{z}{2\sqrt{\alpha t}}\right]\right)\frac{d\beta}{\beta},\end{aligned} \tag{5}$$

for any $r>0, z>0, and\ t>0$. Where J_0 and J_1 are the zero and first order of the Bessel functions. In addition, the exact solutions of z=0 surface and r=0 centerline, is given by

$$\frac{T(r,0,t)-T_0}{q_0 r_p/k}=\int_{\beta=0}^{\infty}\mathrm{erf}\left[\frac{\beta(\alpha t)^{1/2}}{r_p}\right]J_0\left(\frac{\beta r}{r_p}\right)J_1(\beta)\frac{d\beta}{\beta} \tag{6}$$

and

$$\frac{T(0,z,t)-T_0}{q_0 r_p/k}=2\frac{\sqrt{\alpha t}}{r_p}\left[ierf\left(\frac{z}{2\sqrt{\alpha t}}\right)-ierf\left(\frac{\sqrt{z^2+r_p^2}}{2\sqrt{\alpha t}}\right)\right]. \tag{7}$$

The heat flux q_o is given by

$$q_0=\frac{C\cdot E_p}{t_{on}\cdot\pi\cdot r_p^2}, \tag{8}$$

$$E_p=\sum_{t=0}^{n}V(t)I(t)\Delta t \tag{9}$$

where E_p is the pulse energy; $V(t)$ and $I(t)$ are the time series voltage and current data, which can be measured by an oscilloscope; Δt is the sampling interval; t_{on} is the pulse on time, and C is the energy distribution ratio into the electrode.

Assuming that the melted material has been completely removed from the electrode after the discharge, and $(r_m, 0)$ and $(0, z_m)$ are the positions where the temperature reach the melting point T_m at the end of the discharge. Then we can estimate r_m the melted crater radius and z_m the melted crater depth by the measurements of the crater's radius and depth. A system of equations can be formed by substituting T_m, r_m, z_m, q_o and t_{on} in equation (6) and (7), which is given by

$$\begin{cases}T_m=f(r_p,C,Q,r_m,t_{on})\\ T_m=f(r_p,C,Q,z_m,t_{on})\end{cases}. \tag{10}$$

System of equations (10) includes complicate contents, thus, it can only be solved numerically. By solving the equations, the values of the pulse energy distribution ratio C and the plasma radius r_p can be found.

SINGLE SPARK EXPERIMENTS

A. EXPERIMENTAL SETUP

The experiments were conducted on a Panasonic MG-ED72W micro-EDM machine. A Tektronix TPS 2024 oscilloscope (2GHz sampling rate per channel) was used to record the discharge voltage, and the current data was measured by the oscilloscope with a Tektronix CT-1 current probe. A Vecco Digital Instruments Dimension 3100 SPM system was employed to measure the dimensions of the craters.

12 sets of experiments were conducted, and table 2 shows the experimental parameters.

Table 2: Experimental parameters

Workpiece	: Ti-6AL-4V alloy
Tool electrode	: Tungsten rod
Dielectric	: Kerosene
Power supply	: RC circuit
Open circuit voltage	: 70V, 110V
Capacitance	: 10pf, 100pf, 220pf
Workpiece polarity	: +, -

B. MEASUREMENT

To solve equation (10), the measurements of V(t), I(t), t_{on}, r_m and z_m were needed. Fig. 3 includes wave forms of the voltage and current signals in one discharge. V(t) and I(t) were read from the data points between t_1 and t_2, where t_1 was the time start discharge and t_2 was the time stop discharge. The interval between t_1 and t_2 was t_{on} the pulse on time.

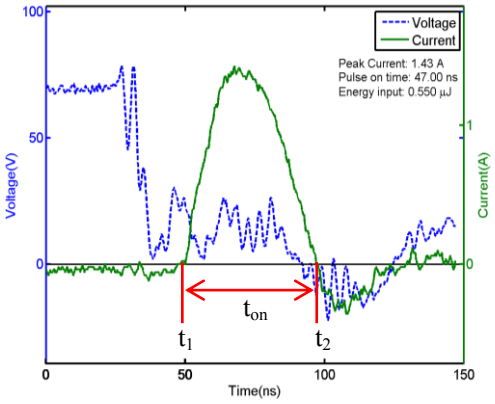

Fig. 3: Wave forms of voltage and current signals

Table 3: ANOVA table of pulse energy

S. V.	SS	DF	MS	F	P-value
Between Groups	0.084	1	0.084	0.92	0.34
Within Groups	5.128	56	0.091		

Table 4: ANOVA table of pulse on time

S. V.	SS	DF	MS	F	P-value
Between Groups	101.8	1	101.8	0.54	0.47
Within Groups	10635.5	56	189.9		

Positive and negative polarities were applied to the workpiece electrodes respectively. Because the materials of the tool and workpiece electrodes were different from each other, we need to test if the pulse energy E_p and the pulse on time t_{on} were affected by these two machining conditions. An ANOVA was used to test if the pulse energy and pulse on time were significantly different between conditions. The P-values of pulse energy in Table 3, and the pulse on time in Table 4 were both larger than 0.05, which indicate that there were no significant differences between the two conditions. Thus, the average values of E_p and t_{on} were used.

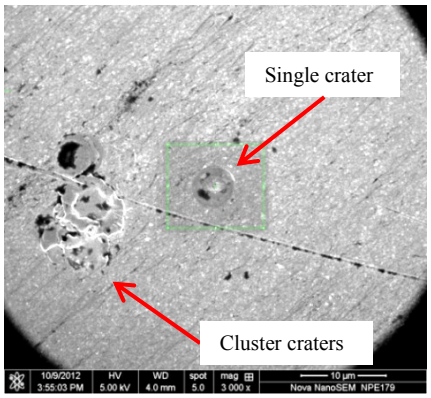

Fig. 4: SEM picture of the area after apply detect surface function

Because the MG-ED72W machine did not have single spark generation function, to obtain a single spark crater, the surface detection function was employed instead. By applying the surface detection function, many craters were generated simultaneously, which include cluster craters and single craters. Fig. 4 shows the surface of the workpiece after conducting the surface detection function, where a single crater and a cluster of craters can be observed. By measuring the single craters on the surface, r_m and z_m can be found.

Fig.5 contains AFM pictures of a crater. Fig. 5(a) is the 3D profile of the crater. Fig. 5(b) is the cross section of the crater. Fig. 5(b) shows the schematic of the measuring of the crater radius r_m and the crater depth z_m.

Table 5: Single spark experimental results

parameters		r_m (µm)	z_m (µm)	E_p (µJ)	t_{on} (ns)	r_p (µm)	C
10pf 70V	+	1.392	0.137	0.090	14.44	1.399	9.7%
	-	0.962	0.093			1.004	4.0%
10pf 110V	+	1.584	0.197	0.191	15.71	1.565	7.9%
	-	1.159	0.122			1.179	3.0%
100pf 70V	+	1.723	0.250	0.211	33.48	1.716	10.9%
	-	1.146	0.147			1.208	3.8%
100pf 110V	+	2.346	0.264	0.378	35.16	2.336	12.0%
	-	1.692	0.217			1.702	5.4%
220pf 70V	+	2.237	0.340	0.573	48.34	2.211	9.1%
	-	1.409	0.128			1.556	2.5%
220pf 110V	+	2.542	0.363	1.020	47.82	2.500	7.0%
	-	2.003	0.155			2.094	2.7%

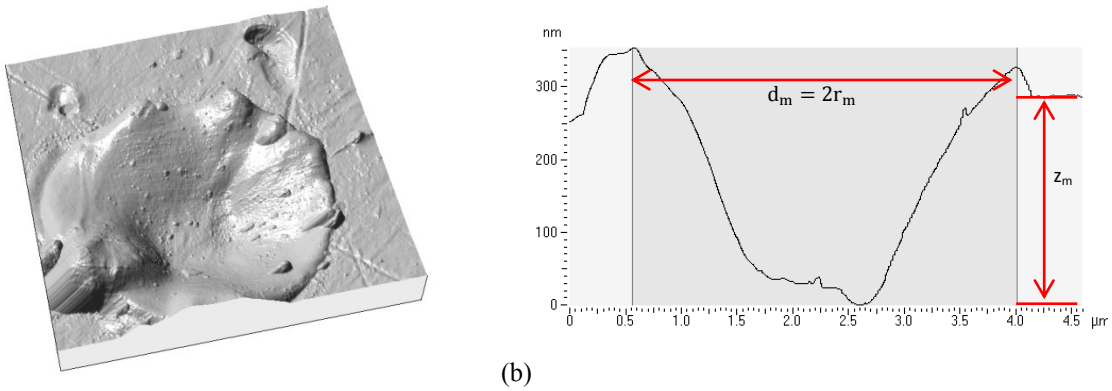

(a) (b)

Fig. 5: AFM pictures of a crater (a) 3D profile of a regular crater, (b) Section of (a)

C. RESULTS

Table 5 lists the measurements and calculations of different machining parameters, where r_m is the measurement of diameter; z_m is the measurement of depth; E_p is the average pulse energy; t_{on} is the average pulse on time; r_p is the calculation of plasma radius and C is the calculation of pulse energy distribution ratio.

Fig. 6 shows the calculation of pulse energy distribution ratio of the anode and the cathode respectively. The average of anode distribution ratio is 9.4% with STD 1.8%, and the average of cathode distribution ratio is 3.6% with STD 1.1%, These values agree with the temperature measurement experimental results reported by M. Zahiruddin et al [10].

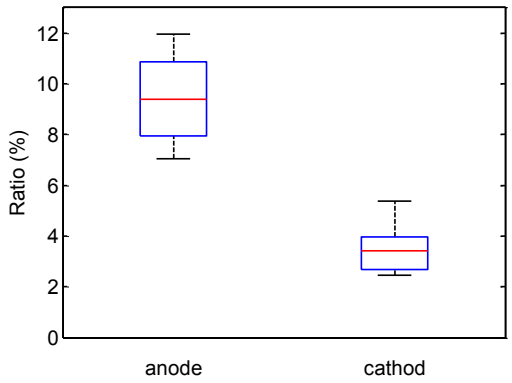

Fig. 6: Pulse energy distribution ratio

ANALYSIS OF EXPERIMENTAL RESULTS

A. INTERRELATION BETWEEN PULSE ENERGY DISTRIBUTION RATIO AND PULSE ENERGY

Fig. 7 plots the relationship between the energy distribution ratio and the pulse energy. The total pulse energy distributes into both electrodes is less than 20%. More than 80% of the total energy is distributed into the inter-electrode gap. This large amount of energy waste is due to the formation of the plasma channel at the beginning of discharge. When the discharge time increases, the plasma channel will approach equilibrium, and more energy will be distributed to the electrodes. In EDM, more than 60% of the pulse energy is distributed into electrodes [7]. Fig. 7 also shows that the pulse energy distributed ratio of the anode is significantly larger than the cathode. Therefore, the polarity of the electrode is a significant parameter of the pulse energy distribution ratio. In addition, the energy distribution ratios are equally distributed from the average ratios for both anode and cathode, respectively. And no data point falls out of the ±3σ limits. When increasing the pulse energy from 0.09μJ to 1.02 μJ, the relationship between the energy distribution ratio and the pulse energy is not significant. In the future, higher pulse energy levels will be applied to investigate the relationship between the energy distribution ratio and the pulse energy.

B. ANALYSIS OF MACHINING PARAMETERS TO THE ENERGY DISTRIBUTED INTO THE ELECTRODES

Fig.8 shows that how much energy has been distributed into the electrodes in different machining parameters. In the figure, with the same machining parameters, energy distributed into the anode is more than the cathode, which is due to the energy distribution ratio of the anode is larger than the cathode. And when open voltage and capacitance increase, more energy is distributed into the electrodes.

C. INTERRELATION BETWEEN ENERGY INPUT AND MATERIAL REMOVAL VOLUME

To analyze the interrelation between energy input and material removal volume, the crater volume needs to be measured. However, the shapes of the generated craters are complicated, which makes the volume hard to measure. Therefore, a simple geometric equation has been applied to approximate the actual crater volume, by assuming the shape of the crater to be a circular parabolic. Then the crater volume is given by

$$V_{\text{crater}} = \frac{1}{2}\pi z_m r_m^2. \quad (12)$$

Fig. 9 illustrates the Energy Utilization Rate (EUR) for both electrodes. EUR is defined as material removal volume per unit energy input. In this figure, generally, the EUR of the anode is higher than the cathode in all machining parameters. The average of anode EUR is 50.6 $\mu m^3/\mu J$ with STD 1 $\mu m^3/\mu J$, and the average of cathode EUR is 38.7 $\mu m^3/\mu J$ with STD 6 $\mu m^3/\mu J$. The EUR variation of the anode is much smaller than the cathode. And from Fig. 9 we can also see that high open voltage leads to a high EUR in cathode.

In Fig. 10 the relationship of the crater volume to the pulse energy has been plotted. The crater volumes of the anode are larger than the cathode. This phenomenon is different from

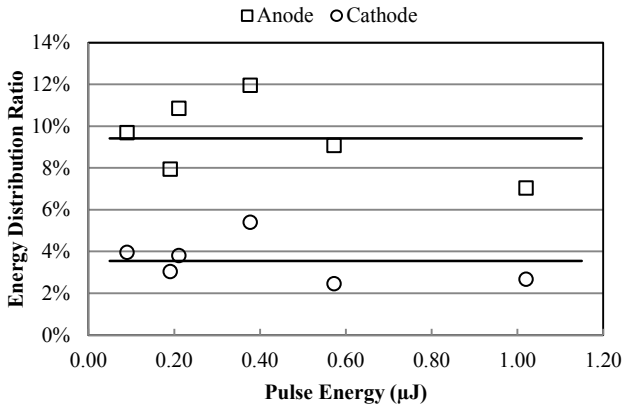

Fig. 7: Relationship between energy distribution ratio and pulse energy

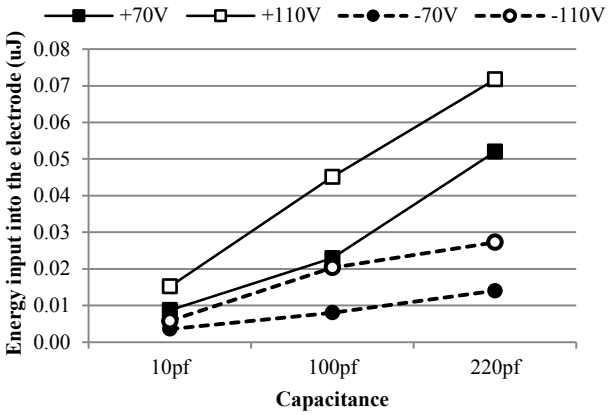

Fig. 8: Energy input into the anode and the cathode with different machining parameters

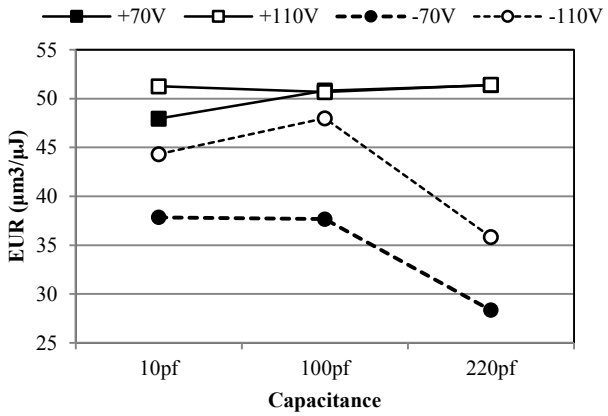

Fig. 9: Energy Utilization Rate of anode and cathode with different machining parameters

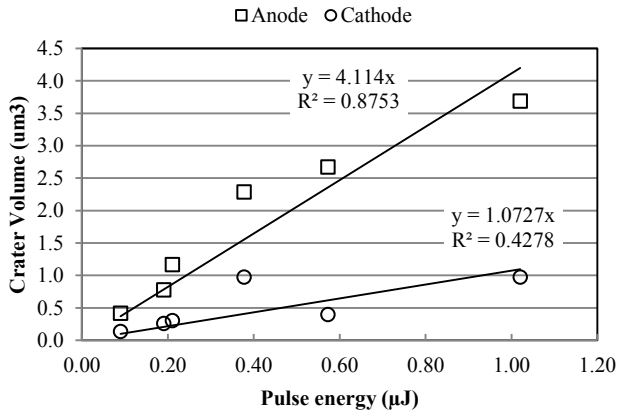

Fig. 10: Linear regression models of crater volume to pulse energy

the EDM with pulse on time longer than 20 µs, where more energy has been distributed to the anode but less material has been removed from the electrode than from the cathode [7]. This is due to the carbon adhesion to the anode electrode surface, where the formed carbon layer will prevent the anode material from been removed. Though, in micro-EDM, carbon adhesion is insignificant. So the input energy should positively correlate to the removed volume from electrode.

The linear regression model of the crater volume to the pulse energy is given by

$$V_{\text{crater}} = \text{EUR} \cdot C \cdot E_p. \quad (13)$$

Fig. 10 gives the linear models for both anode and cathode. The R^2 of the anode model is 0.8753, and of the cathode model is only 0.4278. Thus, the crater volume of the anode is strongly linear dependent on the pulse energy within our experimental pulse energy range. Conversely, the low R^2 value of the cathode model rejects the linear relationship between the crater volume to the pulse energy.

CONCLUSION

In this paper, a method for determining pulse energy distribution ratio in micro-EDM is proposed. Instead of measuring the temperature rise of the electrodes, the dimensions of generated craters have been used to find the pulse energy distribution ratio. This method is easy to apply and do not require mounting any transducers and other special equipment to the machine.

Experimental results show that when the pulse energy is from 0.09 µJ to 1.02 µJ, the average of anode pulse energy distribution ratio is 9.4% and the cathode is 3.6%, respectively. These values agree with other reported EDM literature. Additionally, within the pulse energy range in the experiments, the relationship between the energy distribution ratio and the pulse energy is not significant.

We also find that the Energy Utilization Rate of the anode is very stable. With an average of 50.6 $\mu m^3/\mu J$, which indicates that the crater volume of a single spark is linearly related to the energy input into the electrode. Moreover, with the steady pulse energy distribution ratio, the crater volume of the anode is linearly related to the pulse energy as well. However, the linear relationship between the cathode crater volume to the pulse energy is not as significant as it is to the anode.

ACKNOWLEDGEMENT

Authors acknowledge the partial support from NSF award No.0928873.

REFERENCES

[1] M. Kunieda *et al.*, "Advancing EDM through fundamental

insight into the process," *CIRP Annals-Manufacturing Technology,* 2005; 54: 64-87.

[2] S.H. Yeo *et al.*, "Electro-thermal modelling of anode and cathode in micro-EDM," *Journal of physics.D, applied physics.,* 2007; 40: 2513-2521.

[3] M.R. Patel *et al.*, "Theoretical models of the electrical discharge machining process. II. The anode erosion model," *Journal of Applied Physics,* 1989; 66: 4104-4111.

[4] J. Tao *et al.*, "Modeling of the anode crater formation in electrical discharge machining," *J Manuf Sci Eng Trans ASME Journal of Manufacturing Science and Engineering, Transactions of the ASME,* 2012; 134.

[5] Y. Sarikavak *et al.*, "Single discharge thermo-electrical modeling of micromachining mechanism in electric discharge machining," *Journal of Mechanical Science and Technology,* 2012; 26: 1591-1597.

[6] M. Shabgard *et al.*, "Experimental investigation and 3D finite element prediction of the white layer thickness, heat affected zone, and surface roughness in EDM process," *Journal of Mechanical Science and Technology,* 2011; 25: 3173-3183.

[7] H. Xia *et al.*, "Removal amount difference between anode and cathode in EDM process," *International journal of electrical machining,* 1996; 1: 45-52.

[8] A. Okada *et al.*, "Energy Distribution in Electrical Discharge Machining with Graphite Electrode," *Memoirs of the Faculty of Engineering, Okayama University,* 2000; 34: 19-26.

[9] S. HAYAKAWA *et al.*, "Time variation and mechanism of determining power distribution in electrodes during EDM process," *International journal of electrical machining,* 2001; 6: 19-25.

[10] M. Zahiruddin *et al.*, "Energy distribution ratio into micro EDM electrodes," *Journal of Advanced Mechanical Design, Systems, and Manufacturing,* 2010; 4: 1095-1106.

[11] K.D. Cole *et al.*, Heat conduction using Green's functions, Editor, CRC Press: 2011, 269-280.